Journal of Petroleum Exploration and Production Technology (2019) 9:2811–2830
https://doi.org/10.1007/s13202-019-0655-4

ORIGINAL PAPER - PRODUCTION ENGINEERING

Reservoir characterization using dynamic capacitance–resistance model with application to shut-in and horizontal wells

Mohammad Salehian[1] · **Murat Çınar**[1]

Received: 15 October 2018 / Accepted: 8 April 2019 / Published online: 16 April 2019

Abstract

Capacitance–resistance model (CRM) is a nonlinear signal processing approach that provides information about interwell communication and reservoir heterogeneity. Several forms of CRM have been introduced; however, they would deliver erroneous model parameters if production history involves shut-in period. To address this issue, this study presents a dynamic capacitance–resistance model (D-CRMP), a comprehensive formulation that is capable of handling multiple shut-in periods in different producers. CRM model parameters are representative of the geological information. Accordingly, two geologically identical synthetic examples are used to validate D-CRMP; one including shut-in periods in historical production data of some producers and the other one with all continuously operating wells. Obtaining the same model parameters and the high quality of fitting in both cases proved the reliability of D-CRMP, which allows the utilization of historical data to characterize the reservoir behavior in real cases. Investigation of uncertainty on the fitted model parameters was also performed to demonstrate that confidence intervals are affected mostly by two aspects; permeability distribution and interwell distance. It is shown that though the confidence intervals in the heterogeneous fields are relatively higher than the homogeneous examples, higher permeability and lower producer–injector distance reduce the uncertainty of model parameters in both cases. This study also applies the proposed model in reservoirs with horizontal wells and further examines the impact of well direction and length of the productive interval on the connectivities between wells.

Keywords Capacitance-resistance model · Reservoir characterization · History matching · Waterflood · Shut-in well · Horizontal well

Abbreviations

BHP	Bottom-hole pressure
CMG	Computer modeling group Ltd.
CRM	Capacitance–resistance model
CWI	Cumulative water injection
D-CRMP	Dynamic capacitance–resistance model
ICRM	Integrated capacitance–resistance model
IMEX	Implicit–explicit black oil simulator
IWC	Interwell connectivity
MLR	Multivariate linear regression
MSHW	Multi-segmented horizontal well

List of symbols

L, F, t	Mean length, force, and time, respectively
c_t	Total compressibility (L^2/F)
f_{ij}	Interwell connectivity between injector i and producer j, dimensionless
I	Water injection rate (L^3/t)
J	Productivity index ($L^5/F-t$)
N_p	Cumulative liquid production rate (L^3/t)
n_P	Total number of producers
n_T	Total number of historic time periods
n_I	Total number of injectors
P_{wf}	Well bottom-hole pressure (F/L^2)
q	Total liquid production rate (L^3/t)
R^2	Correlation coefficient
τ	Time constant, t

✉ Mohammad Salehian
mohammadsalehiyan@gmail.com

✉ Murat Çınar

[1] Department of Petroleum and Natural Gas Engineering, Istanbul Technical University, 34469 Maslak, Istanbul, Turkey

Introduction

Waterflooding is known as the most frequently used secondary recovery method due to its proven success ratio, application ease, and cost efficiency (Gözel 2015). Recovery efficiency of a waterflood is highly depended on the sweep efficiency and the ratio of oil–water viscosity (Craig 1971; Gözel 2015). Several studies were conducted to propose a way of estimating reserves, recovery rates, and flood life, which, as Thakur and Satter (1998) states, are the most important goals of a waterflooded reservoir management. Volumetric, empirical and classical methods, performance curve analysis, and numerical reservoir simulation constitute the five common methods used to characterize the waterflood performance.

The capability of interwell connectivities (IWCs) to infer reservoir's geological properties prompted some to present several methods regarding this issue. Heffer et al. (1997) used Spearman rank correlations to detect the relationship between injection–production well pairs and infer them to the geomechanical features of the reservoir. Jansen and Kelkar (1997) investigated the dependence of injection/production rates and pressure on the location of active wells in a waterflooded reservoir. Pizarro (1998) also utilized the Spearman rank method to compare observed data with numerical simulation results and reported the advantages and drawbacks. Soeriawinata and Kelkar (1999) presented a superposition-based approach to resolve the effect of multiple injectors on a single producer by using cross-correlation between the summations of the injection rates with the production rate.

Alejandro and Lake (2002) developed a robust multivariate linear regression (MLR) technique to calculate the connectivity and diffusivity filter (time lag) between injection–production well pairs and estimate the total liquid (oil and water) production of wells, simply using injection and total production rates in waterflood systems. They analyzed the interaction between wells such that water injection and total production, respectively, are regarded as stimulus and response in a reservoir system. Gentil (2005) explained the physical meaning of IWC and examined the relationship between transmissibility and heterogeneity. Dinh and Tiab (2008) extended MLR's application and established a relationship between IWCs and bottom-hole pressure (BHP) in injection and production wells. Although using MLR was a major breakthrough toward estimating IWC within a short time in a practical way, it suffered from some important limitations such as the assumption of constant BHP during the simulation.

Capacitance–resistance model

Yousef et al. (2006) introduced capacitance–resistance model (CRM), a nonlinear data-driven model to estimate the IWCs between production and injection wells within various conditions accurately. CRM considers the effect of capacitance (compressibility) and resistance (transmissibility), which correspond to two parameters, respectively: The degree of fluid storage (time constant, τ) and the degree of connectivity (weight coefficient, f) between wells. By considering injection rates as input data and production rates as output, the CRM is derived based on the total fluid mass balance in the control volume. In addition to synthetic examples, Yousef et al. (2006) validated this approach by applying to real fields.

Sayarpour (2008) and Sayarpour et al. (2009) presented three branches of CRM based on the attribution of model parameters to different control volumes;

- CRMT (control volume is the whole field),
- CRMP (each producer has a drainage volume),
- CRMIP (a control volume for each injector–producer pair).

In producer-based representation of CRM (CRMP), where each producer owns a control volume (Fig. 1), the governing equation is as follows:

$$q_j(t_k) = q_j(t_0)\mathrm{e}^{\frac{-(t_0-t)}{\tau_j}} + \left(1-\mathrm{e}^{\frac{-(t_0-t)}{\tau_j}}\right) \times \left(\sum_{i=1}^{n_1} f_{ij} I_i(t_k) - J_j\tau_j \frac{P^k_{\mathrm{wf},j} - P^{k-1}_{\mathrm{wf},j}}{\Delta t}\right) \quad (1)$$

where $q_j(t_k)$ is the total liquid production of producer j at time step t_k. Equation 1 quantifies three model parameters: τ_j (time constant) for each producer representing the fluid storage in control volume; f_{ij} for each producer–injector pair, showing the magnitude of IWC, and J_j for each producer which determines the effect of producer's BHP on

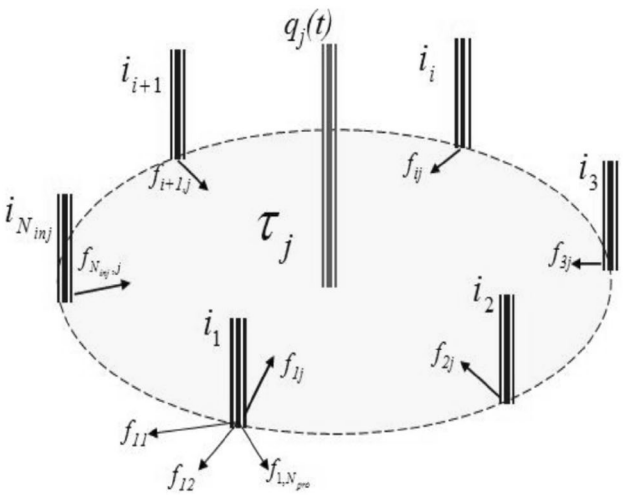

Fig. 1 Schematic representation of CRMP (Sayarpour 2008)

production. In case BHP is not available or assumed to be constant, the CRMP reduces to Eq. 2.

$$q_j(t_k) = q_j(t_0)\mathrm{e}^{\frac{-(t_0-t)}{\tau_j}} + \left(1-\mathrm{e}^{\frac{-(t_0-t)}{\tau_j}}\right)\left(\sum_{i=1}^{n_I} f_{ij} I_i(t_k)\right) \quad (2)$$

Unknown model parameters including f_{ij}, τ_j, and J_j (in case of availability of BHPs) would be estimated via minimizing the error between observed and CRM liquid rates (Eq. 3), if there are n_P number of producers.

$$\min\left\{\sum_{k=1}^{n_\mathrm{T}}\sum_{j=1}^{n_\mathrm{P}}\left(q_{j_{\mathrm{obs}}}(t_k) - q_{j_{\mathrm{CRMP}}}(t_k)\right)^2\right\} \quad (3)$$

Sayarpour (2008) also mentioned that the following constraints should be applied to avoid illogical results.

$$f_{ij}, \tau_j \geq 0 (\text{for all } i \text{ and } j) \quad \text{and} \quad \sum_{j=1}^{n_\mathrm{I}} f_{ij} \leq 1 (\text{for all } i) \quad (4)$$

Kim (2011) presented integrated capacitance–resistance model (ICRM), a linearized form of CRMP, to fit the cumulative total production using cumulative water injection rates as inputs. The ICRM quantifies same model parameters as CRMP.

$$N_{\mathrm{P}_j}(t_k) = \left(q_j(t_0) - q_j(t_k)\right)\tau_j + \sum_{i=1}^{n_\mathrm{I}}\left[f_{ij}\mathrm{CWI}_i(t_k)\right] + J_j\tau_j\left(P^{t_0}_{\mathrm{wf},j} - P^{t_k}_{\mathrm{wf},j}\right) \quad (5)$$

In Eq. 5, $N_{\mathrm{P}_j}(t_k)$ is the cumulative amount of total liquid (oil and water) produced from producer j at time step k. $\mathrm{CWI}_i(t_k)$ is the cumulative amount of water injected by the injector i at time step k. If the BHPs are constant or not available, the simplified version of Eq. 5 is,

$$N_{\mathrm{P}_j}(t_k) = \left(q_j(t_0) - q_j(t_k)\right)\tau_j + \sum_{i=1}^{n_\mathrm{I}}\left[f_{ij}\mathrm{CWI}_i(t_k)\right] \quad (6)$$

Kim (2011) used the same constraints in Eq. 4 to match data and proposed the following objective function to determine model parameters:

$$\min\left\{\sum_{k=1}^{n_\mathrm{T}}\sum_{j=1}^{n_\mathrm{P}}\left(N_{P_{j_{\mathrm{obs}}}}(t_k) - N_{P_{j_{\mathrm{ICRM}}}}(t_k)\right)^2\right\} \quad (7)$$

The objective function (Eq. 7) should be minimized associated with Eqs. 5 or 6 (in case the BHPs are constant) by considering the constraints in Eq. 4. This leads to an MLR analysis in which any local minimum found by Eq. 7 is the global minimum. In previous nonlinear CRMs, as number of model parameters increase or extreme fluctuations present in injection rates, finding global minimum is hard and may lead to erroneous solution by being stuck in unrepresentative local minimum. Using the ICRM, the linear regression provides a unique set of model parameters representing the global minimum and reduces the computation time. Salehian and Soleimani (2018) improved the matching performance of ICRM by employing two consecutive objective functions for both monthly and cumulative liquid production match. Recently, there have been several efforts to characterize layered reservoirs with different types of CRM along with their application into conventional and smart reservoirs (Mamghaderi and Pourafshary 2013; Prakasa et al. 2017; Salehian et al. 2018; Temizel et al. 2018; Zhang et al. 2015, 2017). Nevertheless, there is still lack of information in the application of CRM in shut-in and/or horizontal wells. To address these issues, this paper modifies the classic CRMP presented by Sayarpour (2008) and extends its application to more realistic reservoir and well conditions.

Weber et al. (2009) stated that shut-in periods present a problem for CRM, as it cannot distinguish the zero rate of production due to the shut-in or abandonment in response to possible operational reasons (i.e., extremely low permeable zone, barriers around well, formation damage, etc.). Hence, using these models in reservoirs in which some production wells are shut-in for a specified period or abandonment would result in underestimated connectivities, as optimization skews model parameters downward to account for zero production in given time steps. Kaviani et al. (2012) and Soroush et al. (2014) addressed this issue by modifying the history matching window. Altaheini et al. (2016) presented a modified injection rate as an extra expression to previously proposed models. More recently, however, as de Holanda et al. (2018) explains, it is still necessary to develop a comprehensive approach to address CRM's issue with shut-in periods in production history.

The reservoir models developed in previous studies about CRM only consider the application of the proposed model in vertical wells. To the best of our knowledge, proposed forms of CRM have not yet been tested in reservoirs with horizontal wells. Therefore, application of CRM (D-CRMP in this study) in horizontal wells becomes necessary to certify that CRM successfully characterizes the reservoir dynamic behavior regardless of well configuration.

This study addresses these two issues (i.e., shut-in periods in production history and application of CRM in history matching of horizontal wells) by presenting a modified model, dynamic capacitance–resistance Model (D-CRMP), based on mathematical and physical derivations. We then validate the new model through a heterogeneous field including temporary shut-in periods in different producers. Thereafter, we apply the proposed model for characterizing the reservoirs including horizontal wells to show the ability of CRM in waterflood

characterization regardless of the type of well, and to illuminate the impact of well configuration and its direction (if horizontal wells is used) on model parameters. We also analyze the confidence interval of obtained D-CRMP parameters in both heterogeneous and homogeneous examples to understand their relationship with the physics of the reservoir.

Mathematical derivation of dynamic capacitance–resistance model (D-CRMP)

Throughout the life of a reservoir, as water cut increases, some production wells may be abandoned or temporarily shut-in for technical reasons (Weber et al. 2009). Assuming an arbitrary reservoir (Fig. 2), a number of production wells may be shut-in at time step t_k. Therefore, the set of active producers (i.e., not shut-in by the operator) at time step t_k is defined as

$$\mathcal{A}(t_k) = \left\{ j | q_j(t_k) \neq 0, p_{\mathrm{wf}_j}(t_k) \neq 0 \right\} \quad j = 1, 2, \ldots, n_{\mathrm{P}} \tag{8}$$

Equation 8 expresses that a producer is an active well at time step t_k if it operates with the nonzero rate of production and nonzero BHP. If all producers are operating at time step t_k (i.e., $1 - \mathcal{A}(t_k) = \emptyset$), and assuming that Darcy's equation is valid for the flow between injector i and producer j, the following equation is available:

$$q_{ij}(t_k) = \frac{\bar{k}_{ij}\bar{A}_{ij}}{B\bar{\mu}L_{ij}} \left(P_{\mathrm{wf}_i} - P_{\mathrm{wf}_j} \right)_{t_k} \tag{9}$$

where $\bar{k}_{ij}$ and $\bar{A}_{ij}$, respectively, represent the average permeability and average cross-flow area in the streamline between injector i and producer j, L_{ij} is the distance between injector i and producer j, $\bar{\mu}$ is the average viscosity of the reservoir, B is the formation volume factor (assumed to be constant in the reservoir), $\left(P_{\mathrm{wf}_i}\right)_{t_k}$ and $\left(P_{\mathrm{wf}_j}\right)_{t_k}$ are BHP of injector i and producer j at time step t_k, respectively. To simplify Eq. 8,

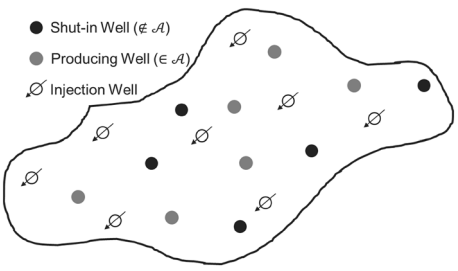

Fig. 2 Schematic representation of an arbitrary reservoir at time step t_k where active and shut-in producers are depicted with gray and black, respectively

one can define the transmissibility between injector i and producer j as follows:

$$T_{ij} = \frac{\bar{k}_{ij}\bar{A}_{ij}}{B\bar{\mu}L_{ij}} \tag{10}$$

Hence, Eq. 9 becomes

$$q_{ij}(t_k) = T_{ij}\left(P_{\mathrm{wf}_i} - P_{\mathrm{wf}_j} \right)_{t_k} = T_{ij}\Delta p_{\mathrm{wf}_{ij}}(t_k) \tag{11}$$

By assuming negligible producer-on-producer effects,

$$I_i(t_k) = \sum_{j=1}^{n_{\mathrm{P}}} f_{ij} I_i(t_k) \tag{12}$$

After substituting the definition of interwell connectivity (Sayarpour 2008), $q_{ij}(t_k) = f_{ij}I_i(t_k)$, Eq. 12 becomes

$$I_i(t_k) = \sum_{j=1}^{n_{\mathrm{P}}} q_{ij}(t_k) \tag{13}$$

and substituting Eq. 11 in Eq. 13 results in

$$I_i(t_k) = \sum_{j=1}^{n_{\mathrm{P}}} T_{ij}\Delta p_{\mathrm{wf}_{ij}}(t_k) \tag{14}$$

Hence, the connectivity between injector i and producer j (Eq. 15) can be determined from Eqs. 11 and 14.

$$f_{ij} = \frac{q_{ij}(t_k)}{I_i(t_k)} = \frac{T_{ij}\Delta p_{\mathrm{wf}_{ij}}(t_k)}{\sum_{j=1}^{n_{\mathrm{P}}} T_{ij}\Delta p_{\mathrm{wf}_{ij}}(t_k)} = \frac{T_{ij}}{\sum_{j=1}^{n_{\mathrm{P}}} T_{ij}} \tag{15}$$

On contrary, if some wells are shut-in at time step t_k (see Fig. 2), the liquid rate between injector i and producer j is given as follows:

$$q'_{ij}(t_k) = T_{ij}\Delta p'_{\mathrm{wf}_{ij}}(t_k) = f'_{ij}I_i(t_k) \tag{16}$$

In these conditions, BHP difference between injector i and producer j depends on $I_i(t_k)$ and T_{ij} of injectors with only active producers ($j \in \mathcal{A}$), such that the summation of all f_{ij} over all active producers is assumed to be equal to unity in a closed system. This assumption is often used in previous forms of CRM to honor the mass conservation in the reservoir, as mentioned in Eq. 4. Hence,

$$\Delta p'_{\mathrm{wf}_{ij}}(t_k) = \frac{I_i(t_k)}{\sum_{j\in\mathcal{A}} T_{ij}} \tag{17}$$

Therefore, Eq. 16 is re-arranged as

$$q'_{ij}(t_k) = T_{ij}\frac{I_i(t_k)}{\sum_{j\in\mathcal{A}} T_{ij}} \tag{18}$$

Based on the derived formulas for $q_{ij}(t_k)$ and $q'_{ij}(t_k)$, the ratio of liquid rate between injector i and producer j, before and after some producers are shut-in, is explained below:

$$\frac{q_{ij}(t_k)}{q'_{ij}(t_k)} = \frac{T_{ij}\Delta p_{\mathrm{wf}_{ij}}(t_k)}{T_{ij}\Delta p'_{\mathrm{wf}_{ij}}(t_k)} = \frac{T_{ij}\frac{I_i(t_k)}{\sum_{j=1}^{n_\mathrm{P}} T_{ij}}}{T_{ij}\frac{I_i(t_k)}{\sum_{j\in\mathcal{A}} T_{ij}}} = \frac{\sum_{j\in\mathcal{A}} T_{ij}}{\sum_{j=1}^{n_P} T_{ij}} = \sum_{j\in\mathcal{A}} f_{ij} \tag{19}$$

$$q_{ij}(t_k) = q'_{ij}(t_k)\sum_{j\in\mathcal{A}} f_{ij} \tag{20}$$

Finally, the connectivity between injector i and producer j, when some producers are shut-in (f'_{ij}) is obtained as follows:

$$f'_{ij} = \frac{q'_{ij}(t_k)}{I_i(t_k)} = \frac{\frac{q_{ij}(t_k)}{\sum_{j\in\mathcal{A}} f_{ij}}}{I_i(t_k)} = \frac{f_{ij}}{\sum_{j\in\mathcal{A}} f_{ij}} \tag{21}$$

In order to use f'_{ij} in CRM formula, an indicator function is used such that

$$\Gamma_j(t_k) = \begin{cases} 1 & j \in A(\text{Active}) \\ 0, & j \notin A(\text{Shut - in}) \end{cases} \tag{22}$$

which shortens Eq. 21 to the following expression

$$f'_{ij}(t_k) = \frac{\Gamma_j(t_k) f_{ij}}{\sum_{\mathcal{J}=1}^{n_\mathrm{P}} \Gamma_{\mathcal{J}}(t_k) f_{i\mathcal{J}}} \tag{23}$$

where $\mathcal{J}$ is used to differentiate from j. Despite previous studies in which the connectivities were assumed as constant parameters, Eq. 23 enables the f_{ij} to act as a dynamic parameter to be turned on or off with respect to the producers' activeness. Substituting Eqs. 1–23 results in the equation of dynamic capacitance–resistance model, D-CRMP (Eq. 24).

$$q_j(t_k) = \Gamma_j(t_k)\left\{ q_j(t_{k-1})\mathrm{e}^{\frac{-\Delta t}{\tau_j}} + \left(1 - \mathrm{e}^{\frac{-\Delta t}{\tau_j}}\right)\left(\sum_{i=1}^{n_\mathrm{I}} \frac{f_{ij}}{\sum_{\mathcal{J}=1}^{n_\mathrm{P}} \Gamma_{\mathcal{J}}(t_k) f_{i\mathcal{J}}} I_i(t_k) - J_j\tau_j \frac{P^k_{\mathrm{wf},j} - P^{k-1}_{\mathrm{wf},j}}{\Delta t}\right)\right\} \tag{24}$$

The indicator function at the beginning of left-hand side would suppress $q_j(t_k)$ to zero, if producer j was shut-in at time step t_k ($j \notin \mathcal{A}(t_k)$). If BHP of all producers is constant, Eq. 24 reduces as follows:

$$q_j(t_k) = \Gamma_j(t_k)\left\{ q_j(t_{k-1})\mathrm{e}^{\frac{-\Delta t}{\tau_j}} + \left(1 - \mathrm{e}^{\frac{-\Delta t}{\tau_j}}\right)\left(\sum_{i=1}^{n_\mathrm{I}} \frac{f_{ij}}{\sum_{\mathcal{J}=1}^{n_\mathrm{P}} \Gamma_{\mathcal{J}}(t_k) f_{i\mathcal{J}}} I_i(t_k)\right)\right\} \tag{25}$$

The previous objective function (Eq. 3) is yet valid for D-CRMP. It is worth noting that if all producers are operating at time step t_k, D-CRMP then reduces to classic CRMP (Eq. 1).

$$\text{if } j = 1, 2, \ldots, n_\mathrm{P} \notin \mathcal{A} \overset{\text{yields}}{\rightarrow} \Gamma_j(t_k) = 1 \forall j = 1, 2, \ldots, \quad n_P \overset{\text{yields}}{\rightarrow} \sum_{j=1}^{n_\mathrm{P}} \Gamma_j(t_k) f_{ij} = 1 \tag{26}$$

The above-mentioned D-CRMP model eliminates shut-in wells at each time step and automatically considers active wells when calculating liquid production rate of each producer. This formulation of dynamic interwell connectivity supports the extra contribution from injection wells (i.e., higher $f'_{ij}(t_k)$) toward active producers, when some other producers are shut-in in a particular time step. The impact of horizontal wells will also be studied through changes in f_{ij} and τ_j relative to the cases where all the wells were vertical.

Results and discussions

In this section, D-CRMP is evaluated for two synthetic reservoirs, identical in all aspects (geological properties, water injection rate history, wells' configuration, and locations), but different in production history, as in the first case all wells operate continuously and the second case includes multiple shut-in periods in different producers. In each case, we apply D-CRMP to characterize the system and match the history of waterflood performance. We focus on the quality of fitting and accuracy of characterization parameters by comparing D-CRMP to the classical CRMP. After validating the new model, we evaluate the capability of CRMs in fully active horizontal wells as well as multi-segmented horizontal wells. In addition, we compare the confidence intervals on estimated parameters within heterogeneous and homogeneous examples.

In this work, commercial reservoir simulator CMG (2017) is used to simulate all synthetic cases, while authors specified all geological information and injection history. Then, a computer code in Python was developed based on the Levenberg–Marquardt algorithm to fit the data.

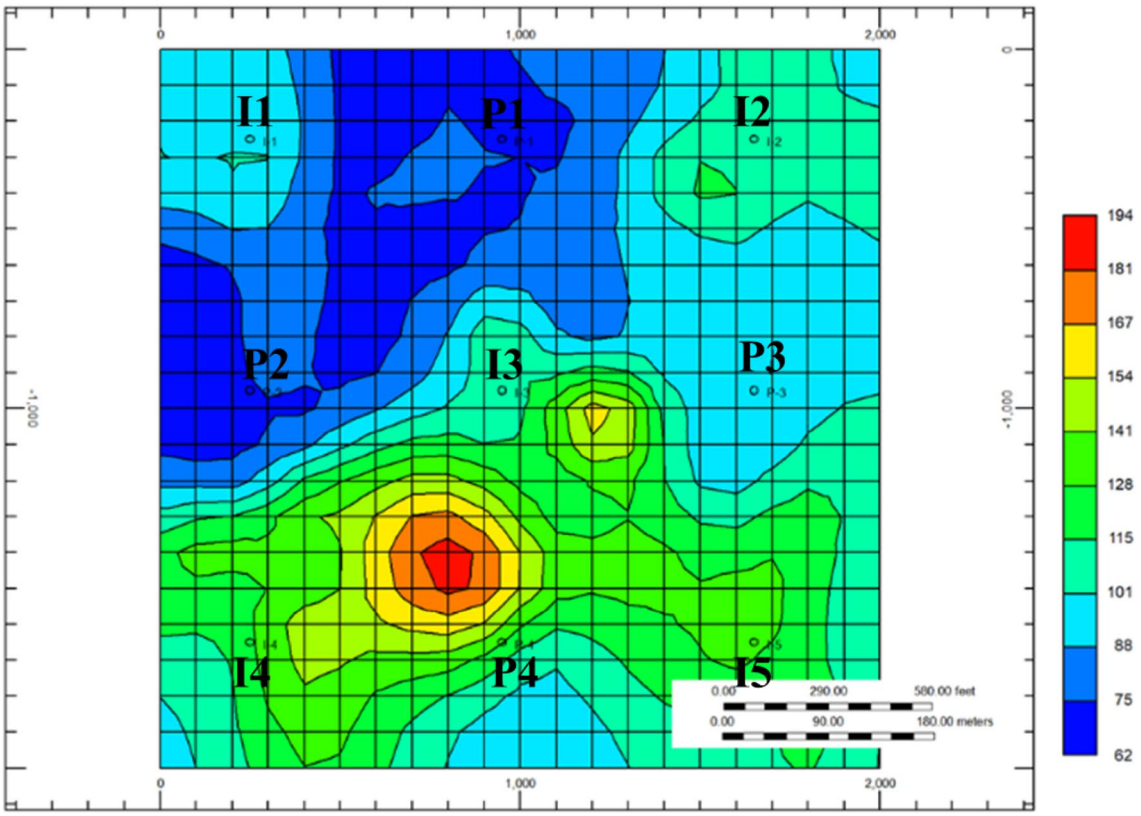

Fig. 3 Permeability distribution in heterogeneous cases I and II (validation of D-CRMP)

We consider a 3D synthetic heterogeneous reservoir where permeability ($k_x = k_y$) is variable in different locations. Figure 3 depicts the 2D permeability distribution in case I (continuous production history) and case II (production history with shut-in periods). The single layer reservoir contains four producers and five injectors with $20 \times 20 \times 1$ grids. The size of the reservoir is $2000 \times 2000 \times 100$ feet and initial pressure of reservoir at the top (5000 feet) is set as 5000 psi. The production and injection are simulated for 8 years (96 months or 2922 days), from January 2003 to January 2011, and BHP of producers is kept constant in 2520 psi.

All synthetic reservoirs contain two phases: water and oil. The oil gravity (API°) is 35, porosity is 21%, formation volume factor is equal to 1.012 bbl/STB, and fluid compressibility is 2.85E−6 l/psi. We assess the performance of D-CRMP based on the accuracy of model parameters and quality of match in two different production scenarios. In case I, producers operate continually, while multiple shut-in periods are implemented in production history of wells in case II.

After validation of D-CRMP in heterogeneous case I and II, we apply it to four homogeneous synthetic reservoirs with horizontal wells to investigate the influence of well direction on IWCs. The production history of horizontal wells has been also involved with shut-in periods. We also consider a reservoir in which the horizontal producer is a multi-segmented well, that is, only some intervals of the well are producing, to study the effect of productive length on CRM outcomes. Finally, we discuss the dependence of model parameters on each other by analyzing the correlation coefficient values.

Validation of D-CRMP

Case I and II are investigated together because they are identical in terms of reservoir properties, injection history, number, location, and configuration of wells. In case I, producers are active during the simulation; however, the production history of case II includes shut-in periods in multiple producers. Figure 4 presents the injection history, where both injection and production start at the beginning of the simulation. Production and injection rates are reported in monthly time steps for 8-year simulation time. It should be noted that this paper does not focus on how wells are controlled or how injection/BHP data are achieved as they are only synthetic input parameters of CRM formulation.

Case I: Heterogeneous field without shut-in periods

The D-CRMP in case I is evaluated in two aspects: agreement of parameters with geological information and the

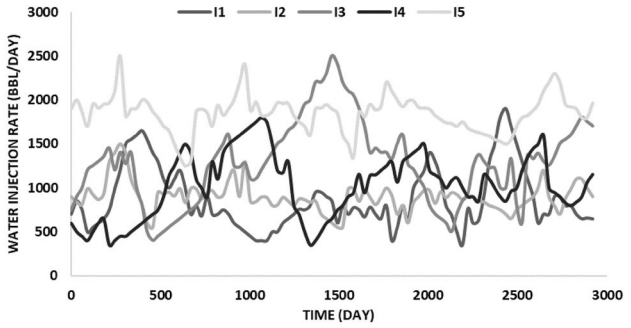

Fig. 4 An example of liquid injection rates in cases I and II. *I*1 stands for injector 1 and others are represented with the same naming convention

quality of the match. As no shut-in period is implemented in this case, D-CRMP acts as classical CRMP. In case I, all time steps are used for verifying the efficiency of D-CRMP. Figure 5 shows the D-CRMP match of the total liquid production (oil and water). The quality of the match is almost perfect as the *R*-squared coefficient of determination (R^2) between the model output and observed (simulation) data varies from 0.98 to 0.99. Figure 6 exhibits the distribution of f_{ij} in case I. It is observed from D-CRMP results that model parameters are in good accordance with the geology of the reservoir. Producers *P*1 and *P*2 that are located in the low permeable region received low connectivities from injectors in the middle and high permeability region. Moreover, injector *I*3 in the center of reservoir contributes more to the producer in high permeability zone (*P*3 and *P*4). All injectors in the corner of the reservoir mostly contribute to the producers nearby, which is in agreement with the fact that f_{ij} decreases as interwell distance increases.

D-CRMP results are validated by using CRMP as a reference model that is proved to be an effective tool for characterizing waterflooded reservoirs. As Fig. 7 depicts, the comparison between D-CRMP and CRMP results reveals that both approaches deliver almost the same connectivities. The minor inequalities between the connectivity values are negligible. Thus, one can certainly conclude that D-CRMP matched liquid production rates effectively and quantified the correct model parameters. In fact, D-CRMP is physically same as CRMP, but including changes in interwell connectivity definition to handle shut-in periods. Thus, same results could be expected in a case with all producers continuously active during simulation. Table 1 presents the estimated model parameters by D-CRMP.

Confidence intervals in heterogeneous case i Uncertainty assessment on model parameters is vital to evaluate the reli-

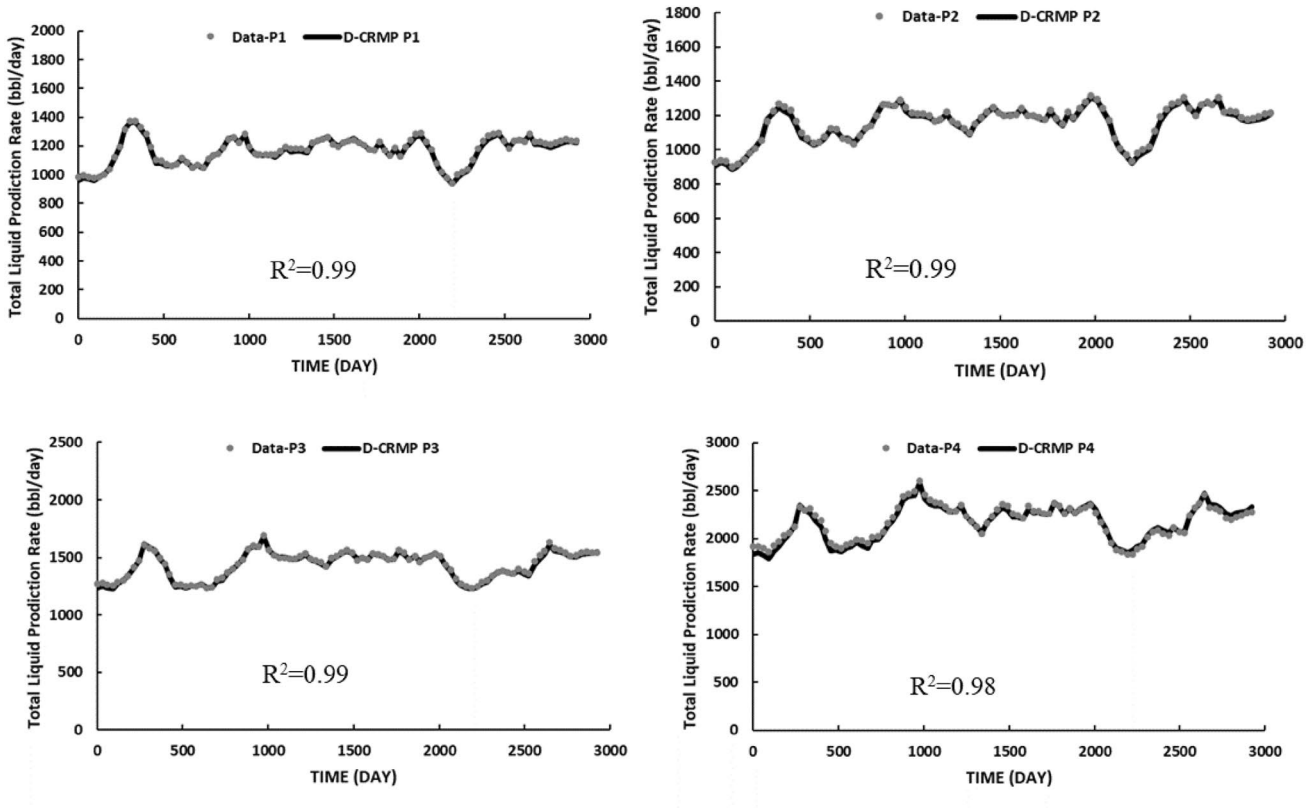

Fig. 5 Liquid production rates match by D-CRMP in case I

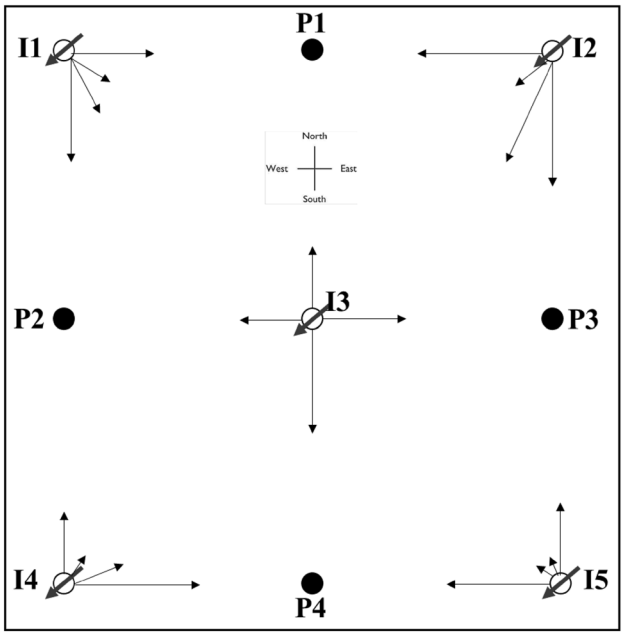

Fig. 6 Distribution of f_{ij} in case I after applying D-CRMP. Each black arrow and its length represent the connectivity and magnitude, respectively

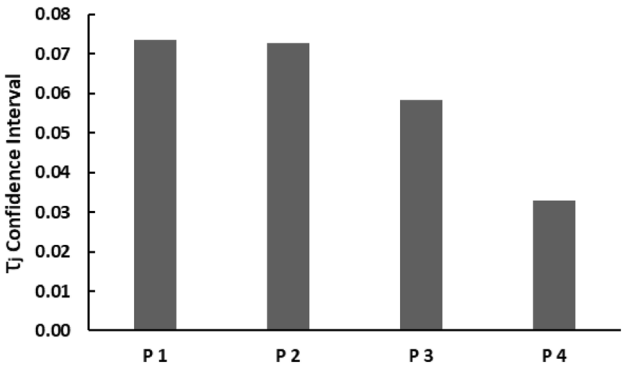

Fig. 8 95% confidence intervals on time constants (τ_j) estimated by D-CRMP in case I. Subscript j stands for the producer index in the range 1 to 4

ability of history matching. In spite of traditional numerical and analytical reservoir models, CRMs are easy to use for statistical analysis. Several approaches such as generating ensembles of history matching results, clustered computing techniques, and Monte Carlo simulations are proposed to study the uncertainty (Landa et al. 2005; Sayarpour 2008). Kim (2011) calculated the confidence intervals for model parameters by both nonlinear and linear regression using Weber (2009)'s method in which time constants are not regression parameters, but constants. In this research, we utilized confidence intervals and correlation coefficients to infer uncertainty on the fitted model parameters. The F-test method was used for calculating confidence intervals to compare our null model, which is the best fit for model parameters, with an alternate model, where one of the parameters is fixed to a specific value.

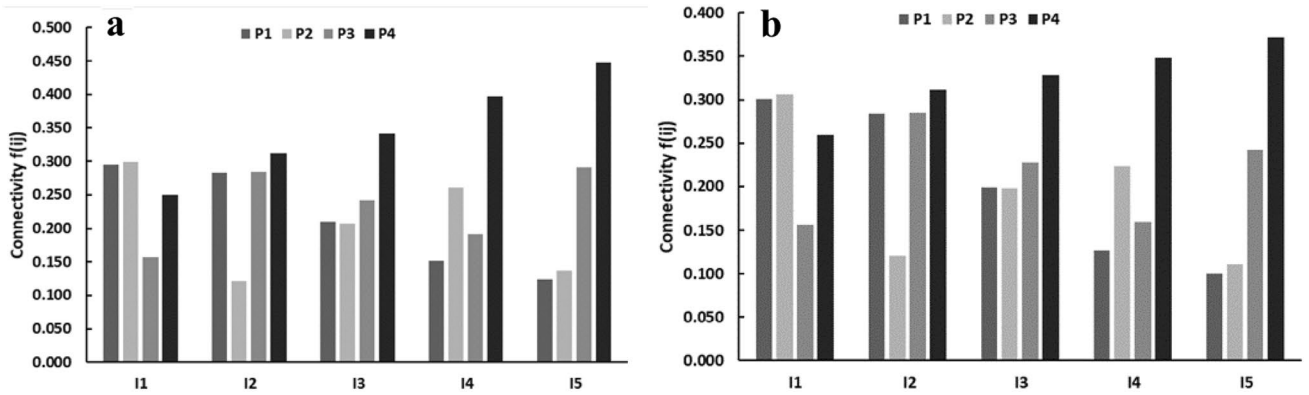

Fig. 7 Connectivities estimated by a) D-CRMP b) CRMP for case I

Table 1 Estimated model parameters by D-CRMP in case I

	τ_j	$I1$	$I2$	$I3$	$I4$	$I5$
$P1$	43.25	0.295	0.283	0.210	0.152	0.124
$P2$	41.31	0.298	0.121	0.207	0.260	0.137
$P3$	43.94	0.157	0.285	0.242	0.192	0.291
$P4$	38.71	0.250	0.312	0.342	0.396	0.448

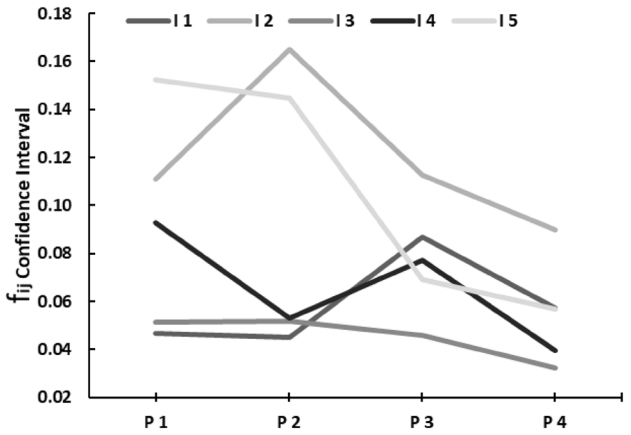

Fig. 9 95% confidence intervals on interwell connectivities (f_{ij}) estimated by D-CRMP in case I. Subscript i and j stand for injector and producer index in range 1–5 and 1–4, respectively

Investigation of confidence intervals reveals that IWCs and time constants are affected by two criteria: (1) permeability distribution and (2) the distance between the producer–injector pair. The confidence interval values of time constants (Fig. 8) of producers $P1$ and $P2$ illustrate higher uncertainty due to the lower permeability zone that they are located. In contrary, $P3$ and $P4$ have received lower confidence interval in such a way that $P4$ has the lowest uncertainty as it is placed in the region with the highest permeability. Thus, one can conclude that the higher permeability has a favorable effect on the uncertainty of time constant.

The 95% confidence intervals of connectivities, shown in Fig. 9, demonstrate the adverse effect of interwell distance on uncertainty. The $I1$ has received lower confidence intervals with $P1$ and $P2$ in f_{11} and f_{12} because they all are in the low permeability zone and near each other. As $I3$ is in the center of the reservoir, almost equal uncertainties are

Table 2 95% confidence intervals of model parameters calculated by D-CRMP in case I

f_{ij}	$I1$	$I2$	$I3$	$I4$	$I5$	τ_j
$P1$	0.0467	0.1110	0.0515	0.0929	0.1525	0.0735
$P2$	0.0452	0.1648	0.0518	0.0529	0.1449	0.0727
$P3$	0.0870	0.1127	0.0457	0.0770	0.0691	0.0583
$P4$	0.0574	0.0898	0.0322	0.0397	0.0567	0.0330

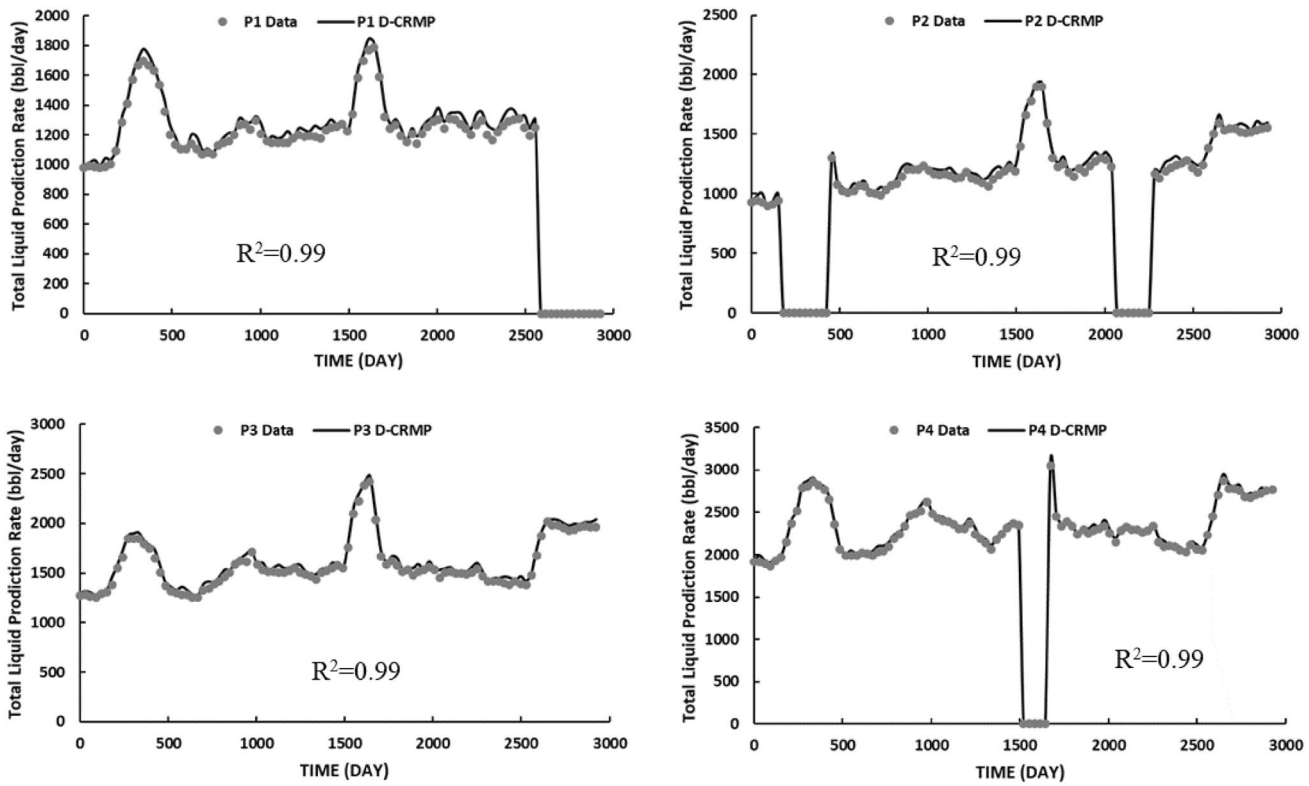

Fig. 10 Liquid production rates match by D-CRMP in case II

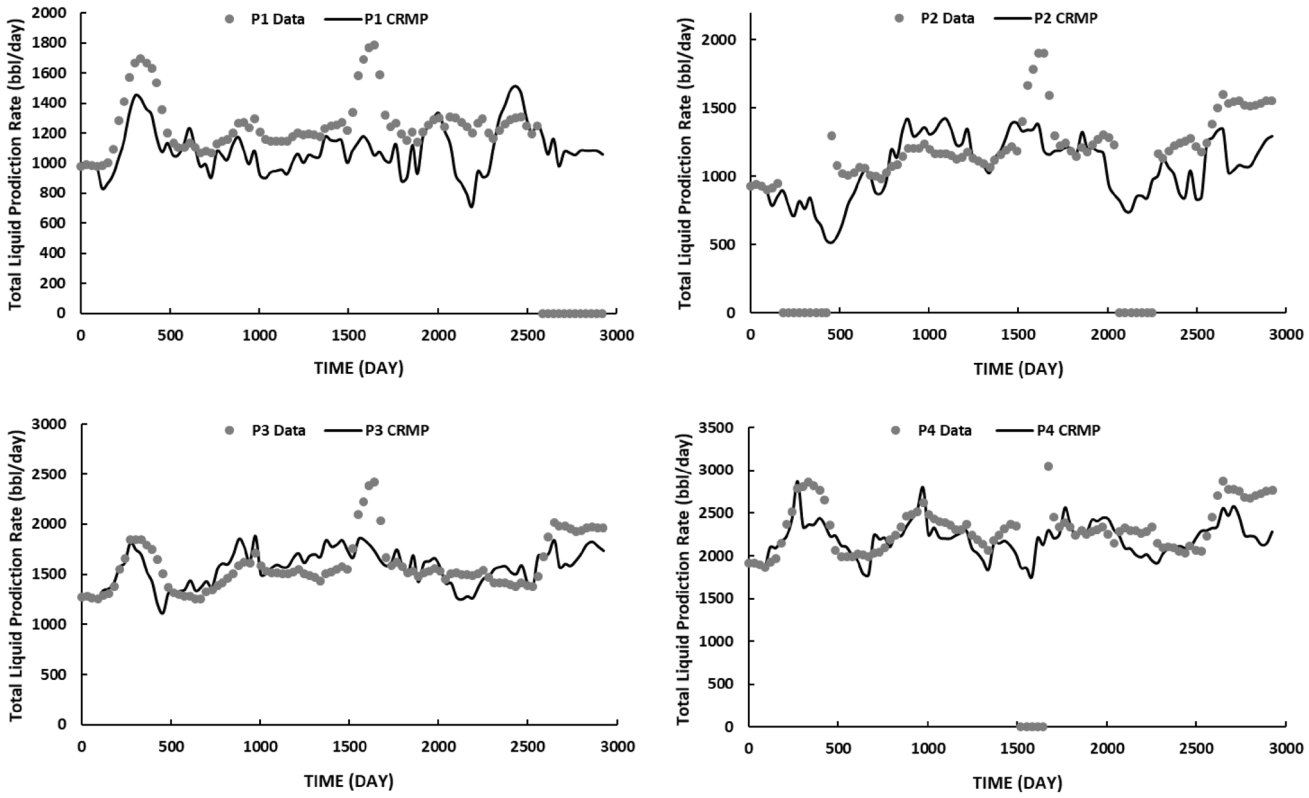

Fig. 11 Liquid production rates match by CRMP in case II

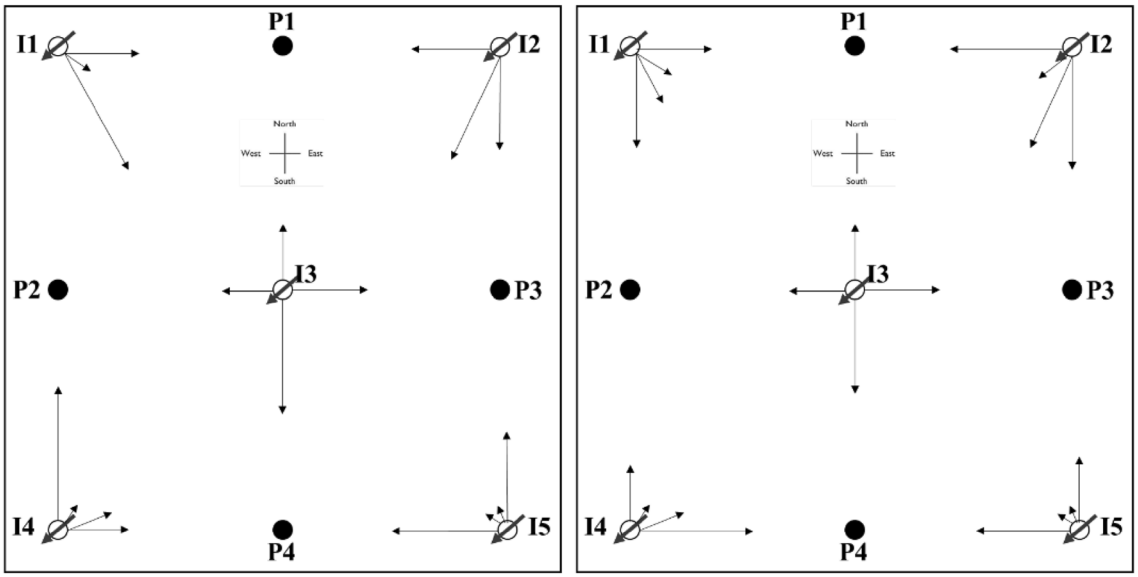

Fig. 12 Distribution of f_{ij} in case II by CRMP (left) and D-CRMP (right). Each black arrow and its length represent the connectivity and magnitude, respectively

obtained for all producers. However, the uncertainties with $P1$ (f_{31}) and $P2$ (f_{32}) are slightly higher because the producers are in the low permeability region. As another instance, $I4$ and $I5$ also have lower uncertainties in connectivities with producers nearby. As producers near $I4$ and $I5$ are all in high permeability zone, both permeability and distance

Table 3 Estimated model parameters by D-CRMP in case II

	τ_j	*I*1	*I*2	*I*3	*I*4	*I*5
*P*1	43.25	0.295	0.283	0.210	0.152	0.124
*P*2	41.32	0.298	0.121	0.207	0.260	0.137
*P*3	43.95	0.157	0.285	0.242	0.192	0.291
*P*4	38.71	0.250	0.312	0.342	0.396	0.448

Table 4 Average reservoir and fluid properties in case III and later

Number of grid blocks	$100\times100\times5$
Size (ft^3)	$2000\times2000\times100$
Horizontal permeability K_h (md)	100
Vertical permeability K_v (md)	20
Porosity (%)	22
Producer bottom-hole pressure constraint (psi)	2000
Reservoir temperature (°F)	158
Oil density (API°)	35
Formation volume factor (bbl/STB)	1.01182
Fluid compressibility (l/psi)	2.85E−6
Formation compressibility (l/psi)	1E−5

have beneficiary effects on the uncertainties. For connectivities of the injector *I*2 (producer *P*1 is near *I*2 but in the lower permeability part) indicates that distance (favorable) and permeability (unfavorable) are acting against each other. In this case, the high difference between the permeability of the regions that the injector *I*2 and the producer *P*1 is located in, resulted in high uncertainty in f_{21}. Lastly, the uncertainty of f_{22} is intensely high due to the fact that the producer *P*2 is both far from the injector *I*2 and located in the low permeability region, while the injector *I*2 is in the higher permeability one. These findings confirm the hypothesis that the higher permeability in the streamline, and the lower distance between producer *j*-injector *i* pair reduces the 95% confidence interval of f_{ij}. Table 2 summarizes the 95% confidence intervals of model parameters (connectivities and time constants) estimated by D-CRMP.

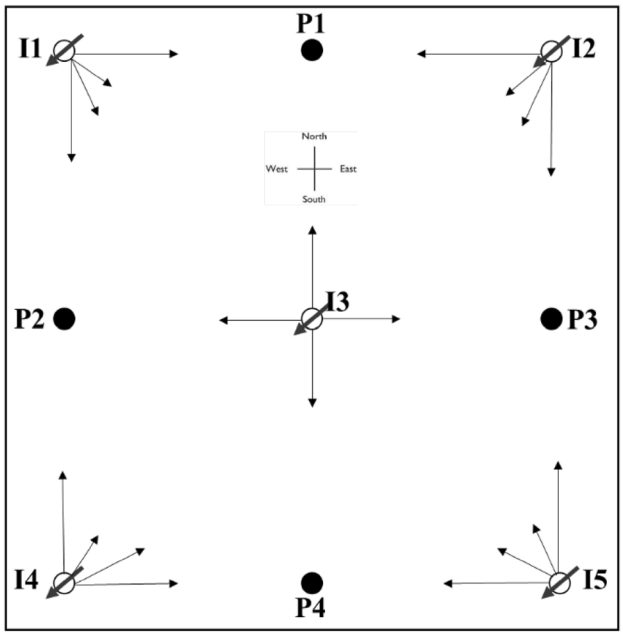

Fig. 14 Distribution of f_{ij} in case III after applying D-CRMP. Each black arrow and its length represent the connectivity and magnitude, respectively

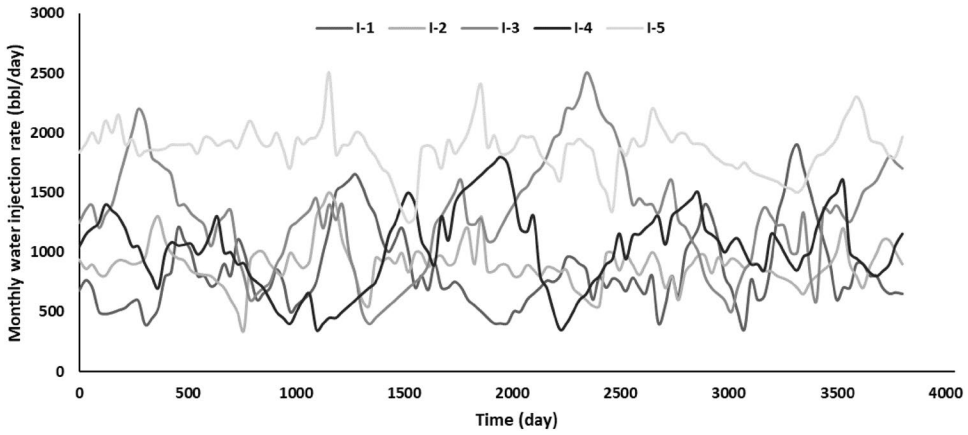

Fig. 13 An example of liquid injection rates in cases III and later. *I*1 stands for injector 1 and others are represented with the same naming convention

Table 5 Estimated D-CRMP parameters for case III

	τ_j	*I*1	*I*2	*I*3	*I*4	*I*5
*P*1	33.873	0.291	0.338	0.253	0.192	0.168
*P*2	35.592	0.322	0.191	0.269	0.325	0.155
*P*3	29.722	0.176	0.271	0.232	0.208	0.348
*P*4	32.634	0.210	0.200	0.246	0.276	0.330

Case II: Heterogeneous field with shut-in periods

In case II, it is assumed that production history involves four shut-in periods that each of them lasts for around 6 months. *P*1 and *P*4 experience one shut-in period and two periods are assumed in production history of *P*2 (i.e., *P*3 operates continuously). The same geology (Fig. 3) and injection rates (Fig. 4) as of case I are used in case II. We aim to validate D-CRMP based on two facts: first, model parameters must be independent of production scenario and second, the quality of liquid production history matching should be acceptable.

As mentioned in the previous section, conventional CRMs such as CRMP and ICRM may not provide completely satisfactory characterizations of model parameters when some producers are abandoned or temporarily shut-in. The inability of those models to distinguish shut-in periods lead to unrealistic and underestimated connectivities due to the wrong interpretation of zero production rates as an indicator of low permeability around the well. This brings the idea of using an improved CRM modification (D-CRMP) based on the producer-based representation of CRM, called CRMP, which was presented by Sayarpour (2008). That is to say, the D-CRMP is insensitive to the number and length of shut-in periods as it eliminates the connectivity of shut-in producers at each time step to avoid illogical results. Hence, in the real cases where some wells might be shut-in by the operator for a while, D-CRMP would be a good choice to characterize the reservoir and forecast the waterflood performance. In this paper, D-CRMP is applied only to characterize the synthetic cases without any production optimization.

This model also works for newly added production wells by assuming them as shut-in wells in the time steps prior to production. Then, they will be treated as normal production

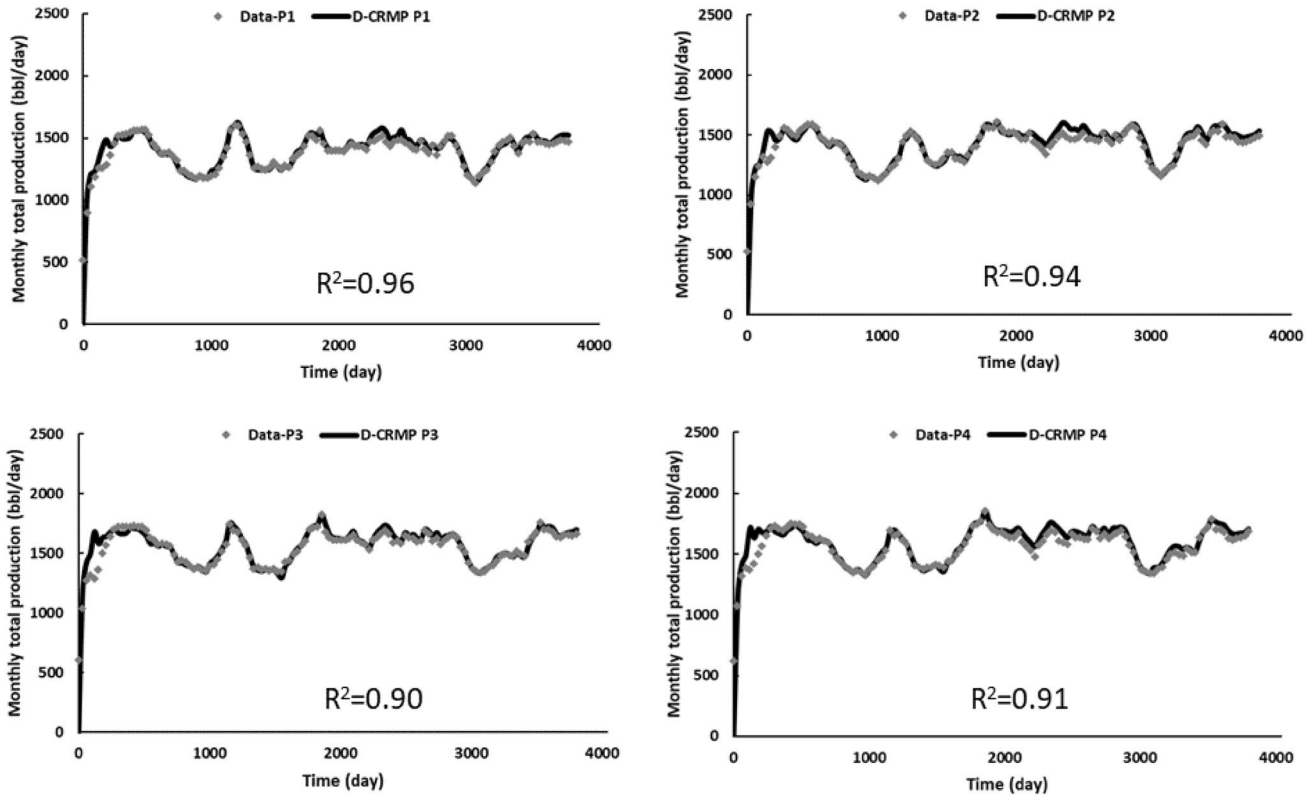

Fig. 15 Liquid production rates match by D-CRMP in case III

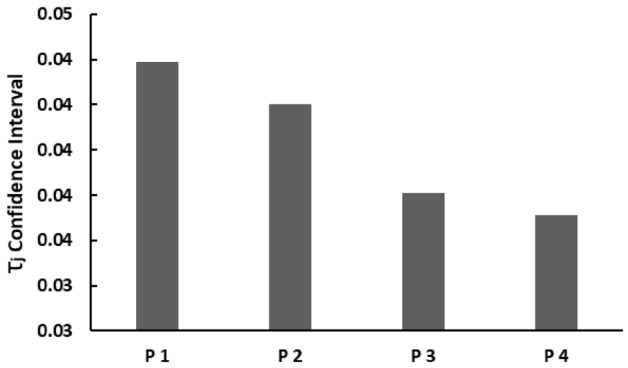

Fig. 16 95% confidence intervals on time constants (τ_j) estimated by D-CRMP in homogeneous case III. Subscript j stands for the producer index in the range 1 to 4

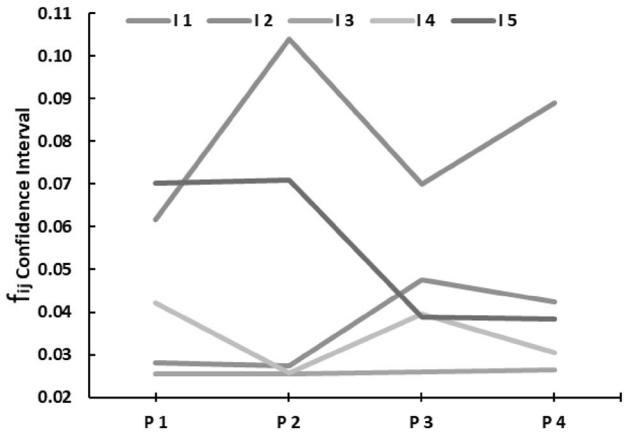

Fig. 17 95% confidence intervals on interwell connectivities (f_{ij}) estimated by D-CRMP in homogeneous case III. Subscript i and j stand for injector and producer index in range 1–5 and 1–4, respectively

wells after being added to the field. The perfect liquid production match by D-CRMP in Fig. 10 associated with high R^2 values illustrates the acceptable performance of this method in matching numerically simulated liquid rates during either active or shut-in time intervals. The poor match in Fig. 11, in contrary, exhibits the failure of CRMP in matching liquid production rates of Case II, even after using a minimal nonzero rate (0.01 bbl/day) during the shut-in periods.

Figure 12 compares the f_{ij} distributions obtained by CRMP and D-CRMP using same fitting window and input data. It is evident from CRMP's results that shut-in periods intensely affected the solution and resulted in unrealistic values. Despite CRMP's failure, D-CRMP shows its independency from production history in such a way that interwell communications and time constants are almost the same as case I's. Estimated model parameters by D-CRMP are given in Table 3. As model parameters obtained by D-CRMP in case I was proved to be in accordance with reservoir properties, true and geology-dependent estimation in case II demonstrates the reliability of this method as an effective tool for characterization of waterflooded reservoirs.

Waterflood history matching in horizontal producers

In this section, we apply D-CRMP to a synthetic homogeneous reservoir including a horizontal well. The reason for choosing a homogeneous reservoir is being able to detect the effect of well configuration in the absence of any other heterogeneity (e.g., permeability, porosity, etc.). Second, we apply our model to the same reservoir, where the horizontal

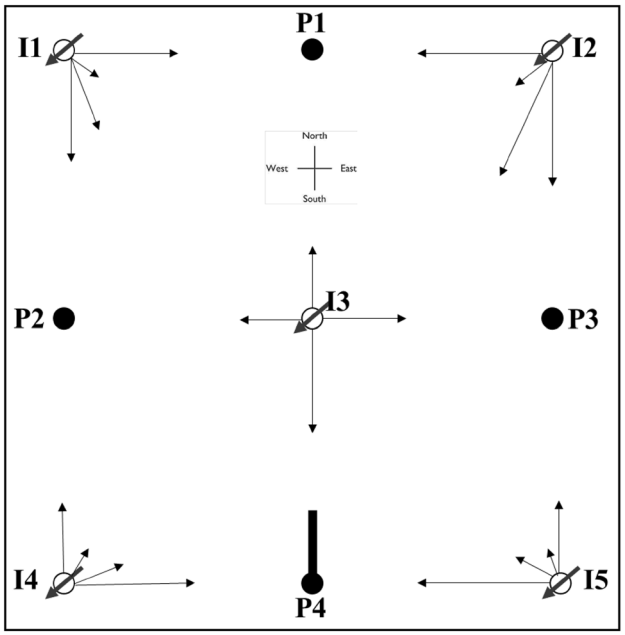

Fig. 18 Distribution of f_{ij} in case IV, where $P4$ is horizontally drilled toward the North. Each black arrow and its length represent the connectivity and magnitude, respectively

Table 6 95% confidence intervals of model parameters calculated by D-CRMP in homogeneous case III

f_{ij}	$I1$	$I2$	$I3$	$I4$	$I5$	τ_j
$P1$	0.0282	0.0617	0.0254	0.0421	0.0701	0.0439
$P2$	0.0275	0.1039	0.0255	0.0257	0.0708	0.0420
$P3$	0.0477	0.0699	0.0260	0.0396	0.0389	0.0381
$P4$	0.0423	0.0889	0.0265	0.0304	0.0384	0.0371

producer is a multi-segmented horizontal well, to investigate the influence of productive length on model parameters. Finally, the impact of the direction of a horizontal well is examined by changing horizontal producer's direction. Note that all reservoir and fluid properties, as well as injection history of studied cases, are identical. We acknowledge that previous forms of CRM may be useable in reservoirs with horizontal wells. However, to our knowledge, the application of a CR model in horizontal wells has not yet been investigated in the literature.

Case III: Basic homogeneous field

A homogeneous synthetic reservoir was built using the commercial simulator, consisting of four vertical producers and five vertical injectors. Table 4 shows the fluid and reservoir characteristics. BHPs of producers are kept constant in all studied cases and the analogous injection history to previous cases (Fig. 13) as of previous part was used in this reservoir. Production starts in January 2000 and lasts until June 2010.

Figure 14 depicts the f_{ij} distribution provided by D-CRMP. The largest connectivities from injector $I1$ is obtained for producers $P1$ and $P2$, suggesting that more than half of the water injected into $I1$ has been travelled toward these two producers. This is because of the low distance between the injector $I1$ and, the producers $P1$ and $P2$. Table 5 illustrates the estimated model parameters. Time constants are approximately equal for all producers due to the homogeneity of the reservoir. The f_{ij} s for other injector–producer pairs are also determined in such a way that more distant pairs receive smaller values. Hence, the obtained model parameters are in good accordance with the imposed geological information. Figure 15 depicts the D-CRMP matching results of liquid production rates, illustrating that the model is perfectly fitted to the production performance.

Confidence intervals in homogeneous case III In this section, we investigate the confidence intervals of model parameters for the homogeneous case III and compare them to those of the heterogeneous case I. It is observed from Figs. 16 and 17 that confidence intervals of time constants and interwell connectivities are similar to heterogeneous case I. Results indicate that as the distance between injector and producer increases, model parameters would be estimated with a higher uncertainty (i.e., higher confidence interval). Table 6 shows the values of 95% confidence intervals of model parameters associated with homogeneous case III. The comparison between Tables 2, 4, and 6 demonstrates that the heterogeneity of the reservoir in case

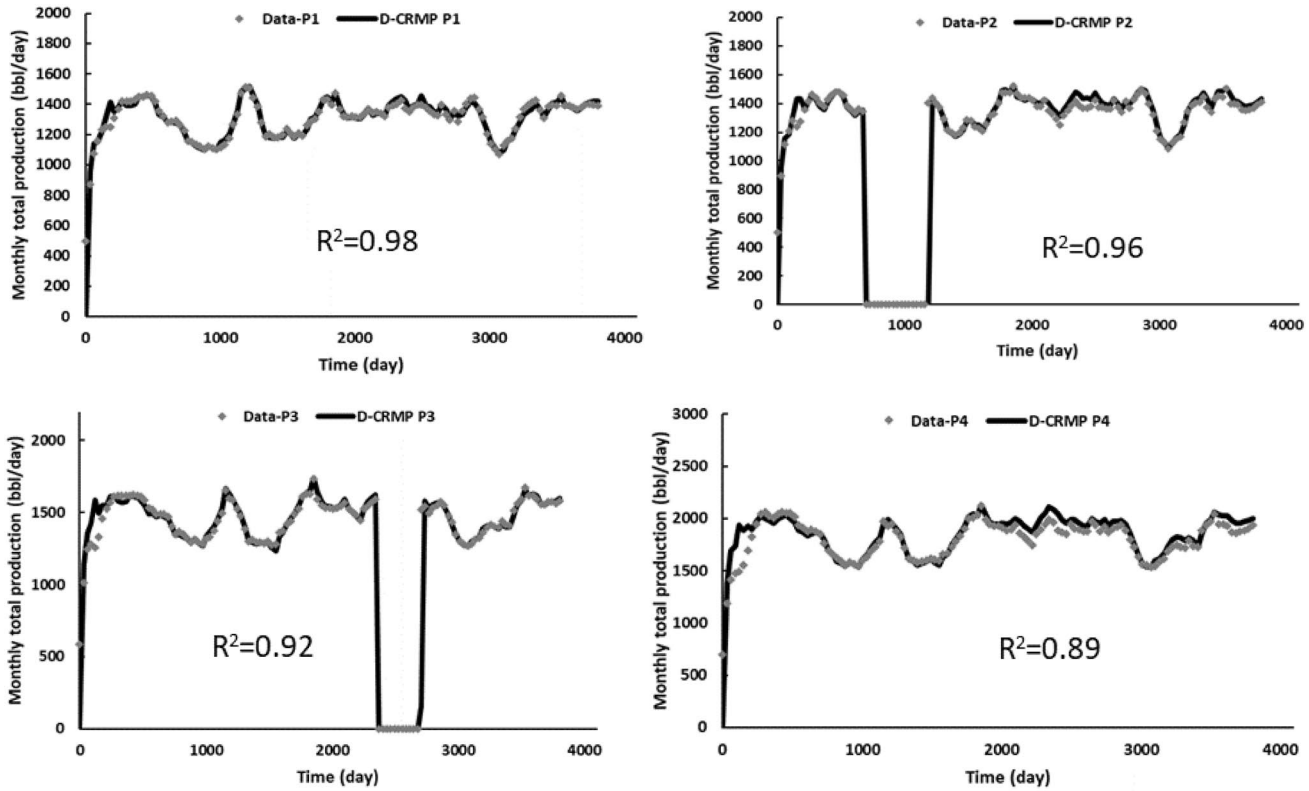

Fig. 19 Liquid production match by D-CRMP for case IV

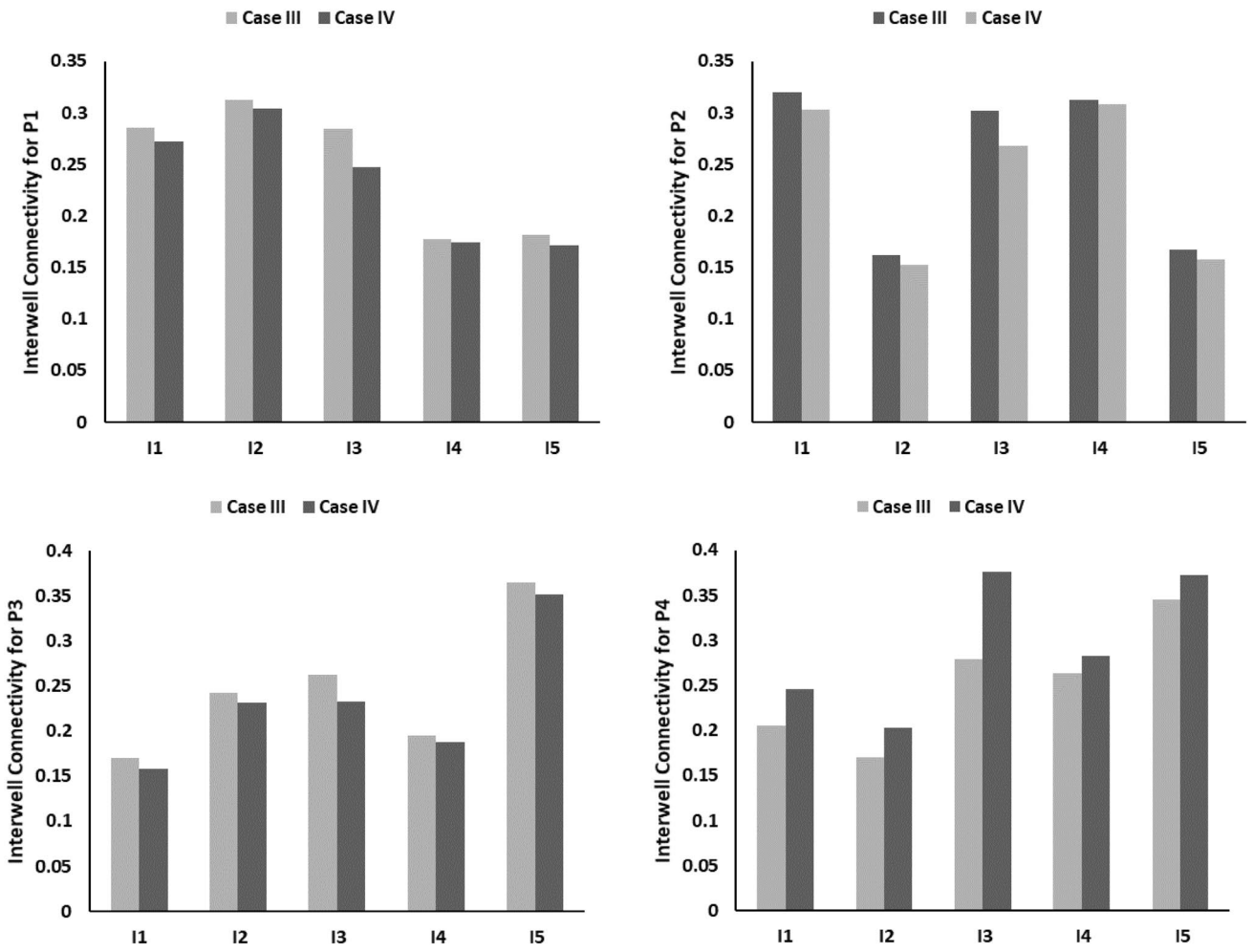

Fig. 20 Comparison between f_{ij} values in case III and case IV

I resulted in an increase in most of the uncertainty values. Thus, one can conclude that though both heterogeneous and homogeneous cases follow the same trend of uncertainties in model parameters, the confidence intervals on model parameters of the heterogeneous case are more uncertain in comparison with the homogeneous field.

Case IV: Horizontal well in North direction

The only difference between case IV and case III (basic reservoir) is the existence of one horizontal producer in *P*4's location which is drilled toward the North in the middle of formation (i.e., 50 ft from the top of the reservoir). The length of the horizontal section is 200 ft and it is fully perforated. Other reservoir and well properties, injection history and fitting window are identical to case III (Table 4).

Figure 18 presents the estimated f_{ij} values by D-CRMP. It is observed that f_{ij} distributions in case IV are different from those results in case III, which is due to the existence of the horizontal production well. Figure 19 shows the results of D-CRMP match for total liquid production rates, where a shut-in period is imposed in production history of *P*3. The high quality of the match in both production and shut-in

Table 7 Estimated D-CRMP parameters for case IV

	τ_j	*I*1	*I*2	*I*3	*I*4	*I*5
*P*1	31.189	0.272	0.304	0.247	0.175	0.172
*P*2	33.637	0.303	0.153	0.268	0.309	0.158
*P*3	27.377	0.158	0.231	0.233	0.187	0.351
*P*4	33.732	0.246	0.203	0.376	0.283	0.373

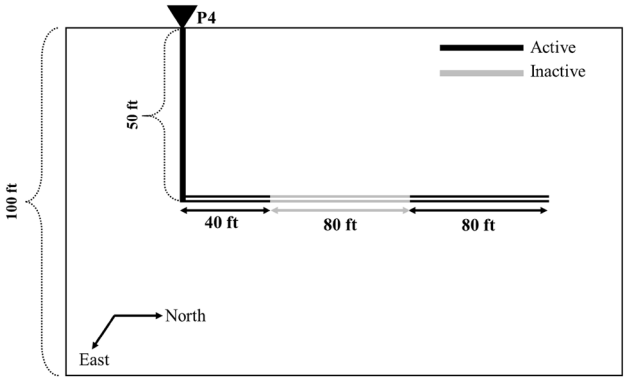

Fig. 21 Schematic view of producer *P*4, a multi-segmented horizontal well in case V

times verifies the success of D-CRMP as an effective tool to match the history of waterflooded reservoirs with horizontal wells.

Figure 20 compares the model parameters of case III (Fig. 12) and case IV. The f_{ij} values between the producer *P*4 and all injectors have increased after changing the *P*4's configuration from vertical to horizontal. The largest improvement is detected in f_{34}, due to the fact that the injector *I*3 is in the same path that the producer *P*4 is drilled. On the other hand, f_{ij} values between all other injector–producer

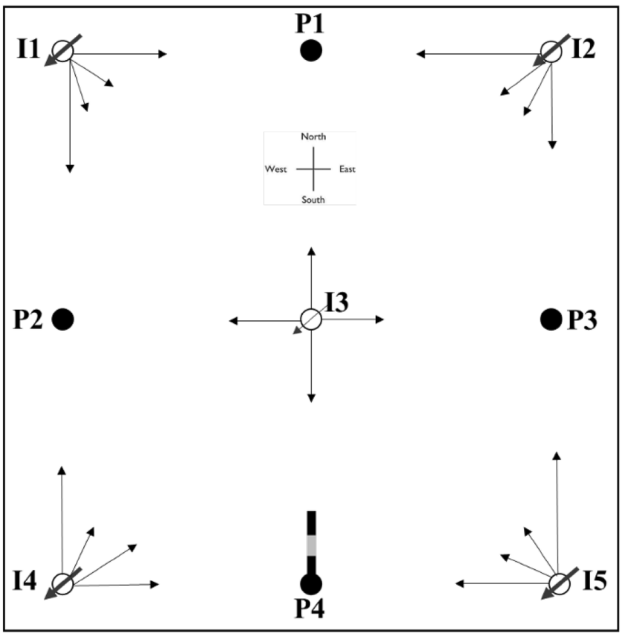

Fig. 23 Distribution of f_{ij} in case V. *P*4 is multi-segmented horizontal well, drilled toward the North. Each black arrow and its length represent the connectivity and magnitude, respectively

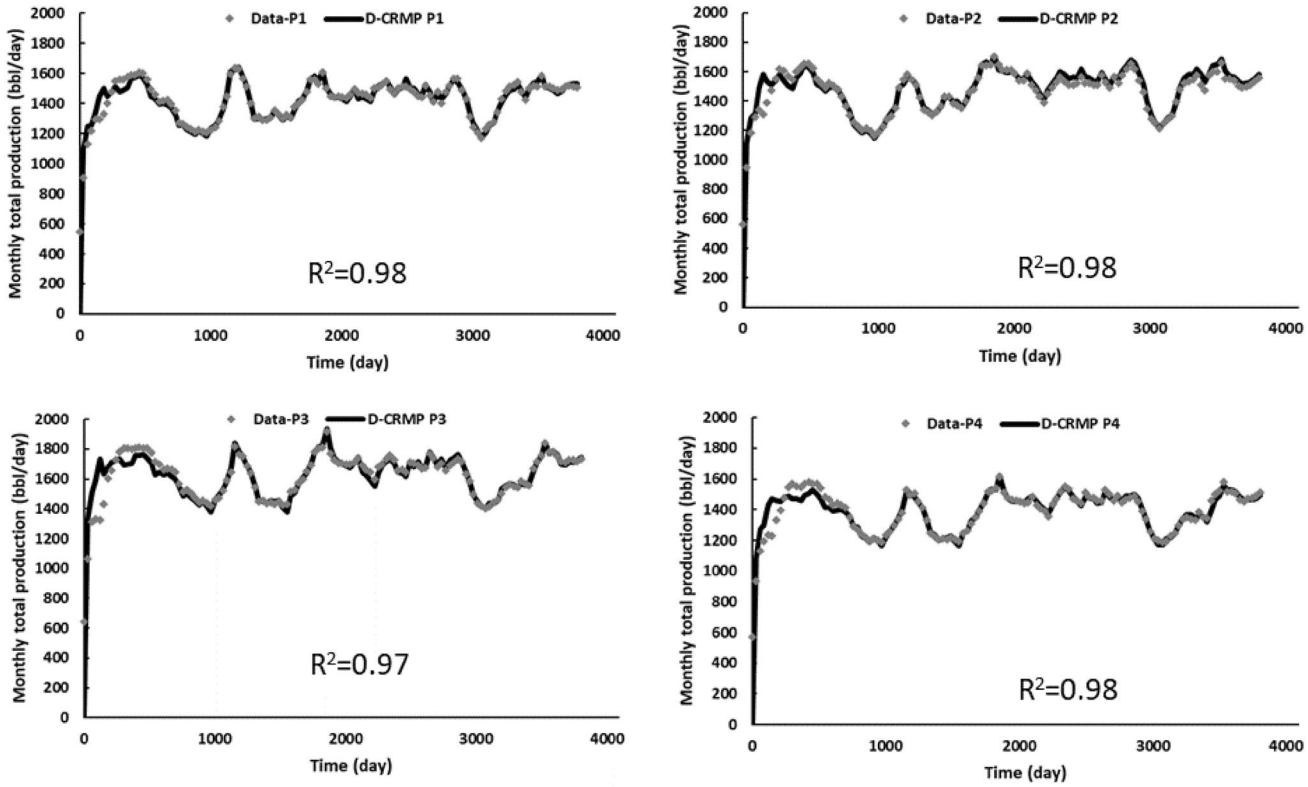

Fig. 22 Total production match by D-CRMP for all producers in case V

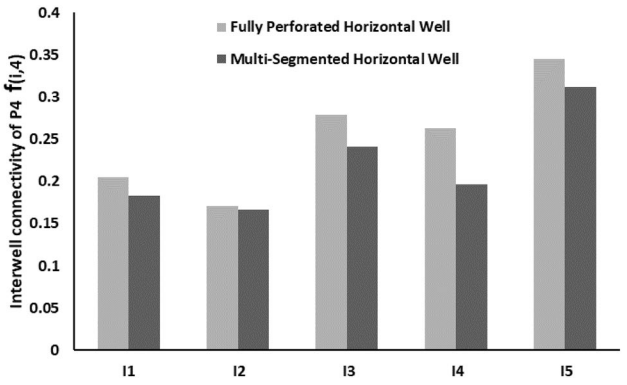

Fig. 24 Comparison of horizontal producer *P*4's IWC in fully perforated (case III) and multi-segmented (case V) conditions

pairs (except *P*4) have decreased. Thus, one can conclude that using a horizontal producer positively affects the interwell connectivities with producers nearby. Examining time constants reveals that using a horizontal producer in the reservoir lead the values of τ to decrease slightly, which might be due to the fact that τ is not affected by well configuration. Table 7 summarizes the estimated model parameters by D-CRMP.

Case V: Multi-segmented horizontal well

In this case, the horizontal producer *P*4 acts as a multi-segmented well which is drilled toward the North. The producer *P*4 is horizontally drilled in the middle layer of the reservoir with the length of 200 ft comprising a 40 ft productive, 80 ft nonproductive and an 80 ft productive interval, respectively. Figure 21 represents the schematic view of the producer *P*4. Like previous cases, same injection data (Fig. 13), reservoir and fluid properties are used in this case (Table 4).

Figure 22 depicts the results of total liquid production match by D-CRMP, which are acceptable. It should be pointed out that the quality of match in the first months of production might be not as good as the rest of reservoir life. This is due to the instability of the flow between wells when production and water injection start at the same time (beginning of the simulation) and pseudo-steady state flow has not been reached yet. Nevertheless, the stable flow data from the rest of reservoir life were enough to obtain perfect fit.

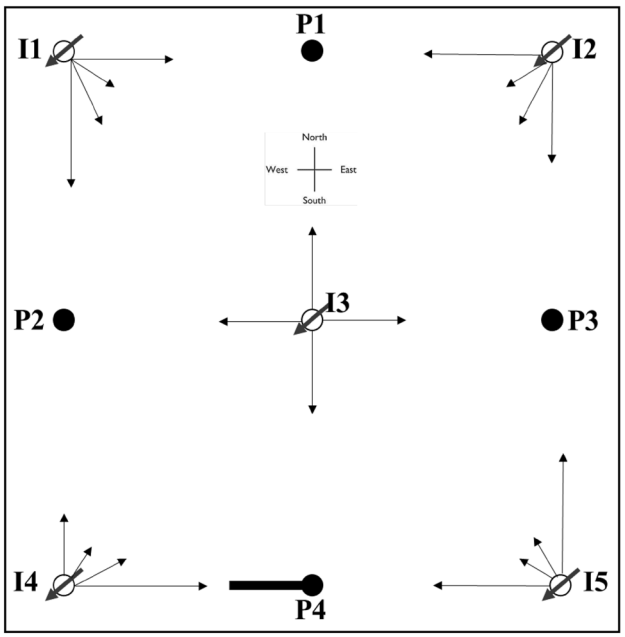

Fig. 25 Distribution of f_{ij} in case VI after applying D-CRMP. *P*4 is horizontal well, which is drilled toward the West. Each black arrow and its length represents the connectivity and magnitude, respectively

Figure 23 shows the f_{ij} distribution in which gray thick line in *P*4 represents the inactive interval of a multi-segmented horizontal well.

Figure 24 compares the f_{i4} ($j = 4$) in fully active and multi-segmented conditions. It is observed that the partially active horizontal production well receives less contribution from other injectors compared to a fully active horizontal producer, which accounts for the adverse effect of the nonproductive interval in *P*4 on production performance and communication with injectors. The comparison between the time constants of producers in fully active and multi-segmented conditions, however, illustrates no remarkable difference. Remembering the slight variation between time constants of case III and case IV also confirms this hypothesis that changing configuration of a well though affects IWCs, it may have nothing to do with time constants in a homogeneous waterflooding system. Table 8 presents the estimated model parameters obtained by D-CRMP.

Table 8 Estimated D-CRMP parameters for case V

	τ_j	*I*1	*I*2	*I*3	*I*4	*I*5
*P*1	30.040	0.301	0.331	0.249	0.208	0.188
*P*2	33.414	0.326	0.173	0.269	0.358	0.186
*P*3	25.283	0.186	0.260	0.225	0.230	0.386
*P*4	30.233	0.183	0.167	0.242	0.196	0.312

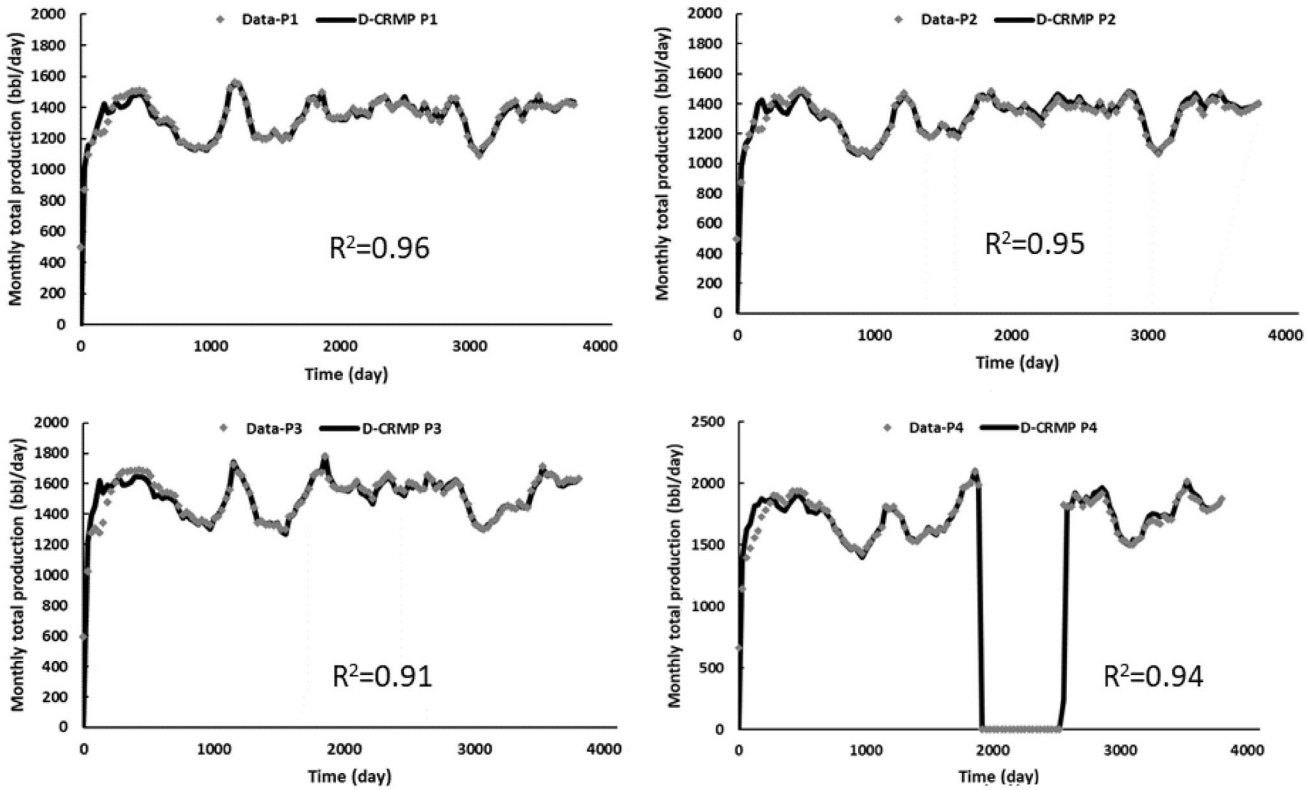

Fig. 26 Total production match by D-CRMP for all producers in case VI

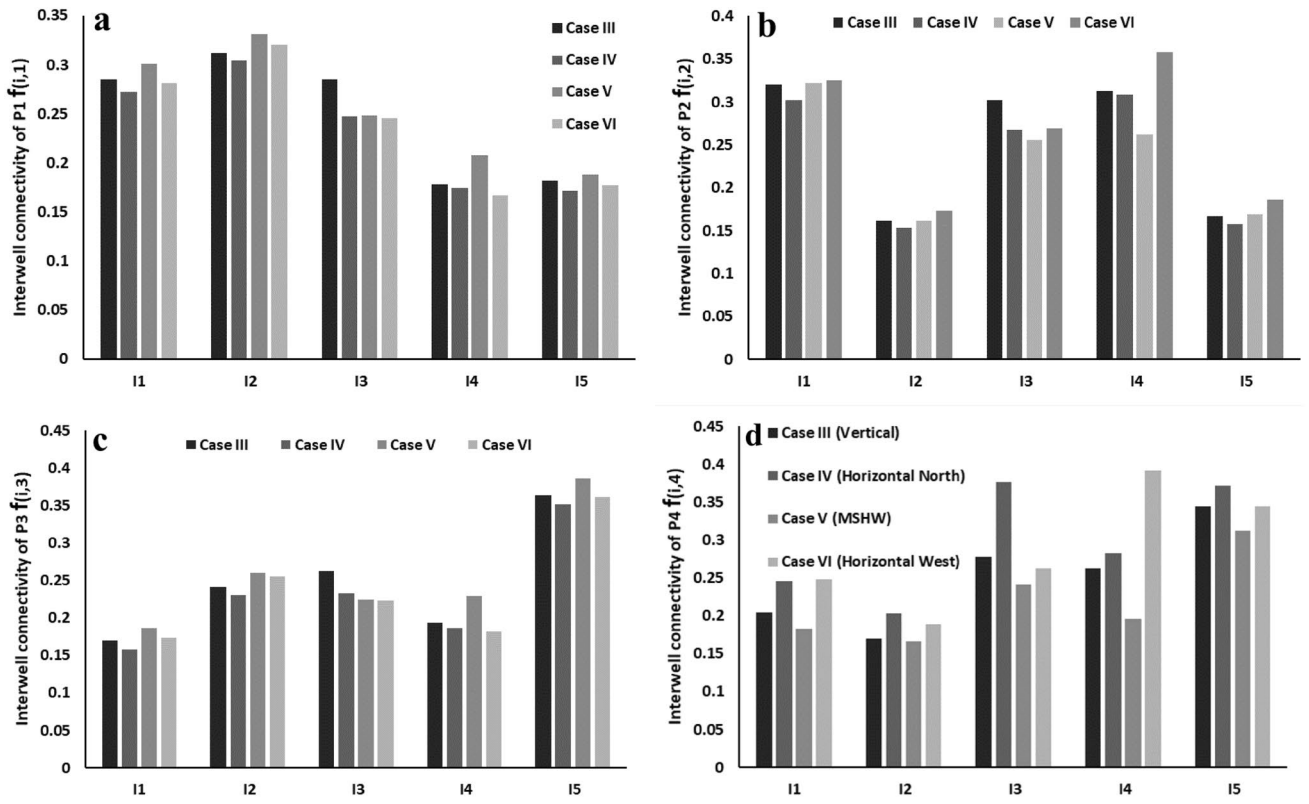

Fig. 27 Comparison between interwell connectivities for *P*4 in case III to VI

Table 9 Estimated model parameters by D-CRMP in case VI

	τ_j	$I1$	$I2$	$I3$	$I4$	$I5$
$P1$	28.436	0.281	0.321	0.245	0.166	0.177
$P2$	30.394	0.322	0.162	0.256	0.262	0.169
$P3$	24.143	0.174	0.255	0.223	0.182	0.361
$P4$	27.348	0.248	0.189	0.263	0.393	0.344

Case VI: Horizontal well in West direction

Another parameter that may affect model parameters is the direction of the horizontal well. In case VI, it is assumed that producer $P4$ is a fully perforated (i.e., fully productive) horizontal well which is drilled toward the West. This provides a good comparison between D-CRMP parameters when the well direction changes from North (case IV) to the West. The horizontal well $P4$, with the same length as in case IV (200 ft), is drilled in the middle layer of the formation. The injection scenario and reservoir characteristics are the same as in previous cases. Figure 25 depicts the f_{ij} distribution obtained by D-CRMP. Figure 26 shows the D-CRMP match of the total liquid production rates. As it was seen in case IV and case V, high values of R^2 validates the model's applicability for reservoirs with horizontal producers.

Figure 27 compares f_{ij} values between case III, IV, V and VI. Generally, horizontal producers have higher productivity index compared to vertical wells. Figures 26b, c and 27a show that producers $P1$, $P2$ and $P3$ would have lower connectivities with other injectors when fully active horizontal $P4$ in either North or West direction was used, which means that existence of a horizontal producer in the reservoir has reduced the contribution of injectors to other producers. On the other hand, it is evident that using a multi-segmented horizontal well increased the connectivity between other producers with injectors $I4$ and $I5$, which are close to MSHW.

It is observed from Fig. 27d that $P4$ has the minimum connectivity when it is a multi-segmented horizontal well, which means that inactivity of certain intervals decreases the connectivity of the well with other injectors. The connectivity values of $P4$ in horizontal conditions, either in the North or West direction, are more than those of vertical condition. This indicates that using a horizontal configuration increases the chance of receiving fluid flowing from other injectors. In this context, $P4$ receives the maximum contribution from $I3$ to $I4$, when it is in North and West, respectively. This is because the injectors $I3$ and $I4$ are located in the same path as $P4$'s direction in each case. Thus, the f_{ij} between a horizontal producer and injector would be larger if the injector stays on the same path of the producer's direction. Table 9 summarizes the model parameters obtained by D-CRMP.

As observed in previous cases, time constants, nevertheless, seem to be insensitive to the direction of the horizontal producer. It is worth mentioning that even though obtained model parameters are similar for different well configurations, they are not exactly same. Nevertheless, all of them can offer an acceptable match of geological information.

Conclusions

The main objectives of this study were to develop the modified version of CRM to characterize waterflooded reservoirs including multiple shut-in periods in production history and utilize the proposed model in reservoirs with horizontal wells. We applied the new model D-CRMP to several heterogeneous synthetic cases and validated its consistency with the imposed geological information. We report that the D-CRMP is an effective tool to obtain realistic insight into the reservoir characteristics and production performance when production data includes shut-in periods. The application of D-CRMP in future prediction and production forecast is recommended as a potential future work.

The analysis of confidence intervals on estimated model parameters showed that the higher permeability and lower interwell distance affects the uncertainty positively. We obtained lower uncertainty for the connectivities of injector–producer pairs in the higher permeability regions as well as those pairs with lower interwell distance. Results also demonstrated higher uncertainty on model parameters in heterogeneous examples in comparison with the similar homogeneous case.

This paper presents informative facts about application of CRMs in waterflooded reservoirs containing horizontal wells. We validated that D-CRMP can match the production rates perfectly. It was also shown that using a horizontal well instead of a vertical well improves the connectivities of the well, especially with those injectors on the same path of the horizontal producer. In addition, application of D-CRMP to a reservoir with multi-segmented horizontal well indicated that a fully productive horizontal well receives larger connectivity values with other injectors compared to a multi-segmented (partially productive) one. Nevertheless, no big differences were observed between the time constants of vertical and horizontal wells with different characteristics, which mean that the type of well configuration does not affect time constants remarkably.

Acknowledgements Authors deeply appreciate Computer Modeling Group (CMG) for donating the license of CMG 2017.

References

Alejandro A, Lake LW (2002) Inferring interwell connectivity from well-rate fluctuations in waterfloods. In: SPE/DOE improved oil recovery symposium. Society of Petroleum Engineers

Altaheini S, Al-Towijri A, Ertekin T (2016) Introducing a new capacitance–resistance model and solutions to current modeling limitations. In: SPE annual technical conference and exhibition. Society of Petroleum Engineers

CMG I (2017) Advanced OI/gas reservoir simulator version 2017 user's guide. Computer Modelling Group LTD, Calgary

Craig FF (1971) The reservoir engineering aspects of waterflooding, vol 3. HL Doherty Memorial Fund of AIME, New York

de Holanda RW, Gildin E, Jensen JL (2018) A generalized framework for capacitance resistance models and a comparison with streamline allocation factors. J Petrol Sci Eng 162:260–282

Dinh AV, Tiab D (2008) Interpretation of interwell connectivity tests in a waterflood system. In: SPE annual technical conference and exhibition. Society of Petroleum Engineers

Gentil PH (2005) The use of multilinear regression models in patterned waterfloods: physical meaning of the regression coefficients. University of Texas at Austin, Austin

Gözel ME (2015) The use of capacitance–resistive models for estimation of interwell connectivity and heterogeneity in a waterflooded reservoir: a case study. Middle East Technical University, Ankara

Heffer KJ, Fox RJ, McGill CA, Koutsabeloulis NC (1997) Novel techniques show links between reservoir flow directionality, earth stress, fault structure and geomechanical changes in mature waterfloods. SPE J 2:91–98

Jansen F, Kelkar M (1997) Application of wavelets to production data in describing inter-well relationships. In: SPE annual technical conference and exhibition. Society of Petroleum Engineers

Kaviani D, Jensen JL, Lake LW (2012) Estimation of interwell connectivity in the case of unmeasured fluctuating bottomhole pressures. J Petrol Sci Eng 90:79–95

Kim JS (2011) Development of linear capacitance–resistance models for characterizing waterflooded reservoirs. M.Sc. dissertation, University of Texas, Austin

Landa JL, Kalia R, Nakano A, Nomura K, Vashishta P (2005) History match and associated forecast uncertainty analysis-practical approaches using cluster computing. In: International petroleum technology conference. International Petroleum Technology Conference

Mamghaderi A, Pourafshary P (2013) Water flooding performance prediction in layered reservoirs using improved capacitance–resistive model. J Petrol Sci Eng 108:107–117

Pizarro JOdSA (1998) Estimating injectivity and lateral autocorrelation in heterogeneous media. University of Texas at Austin, Austin

Prakasa B, Shi X, Muradov K, Davies D (2017) Novel application of capacitance–resistance model for reservoir characterisation and zonal, intelligent well control. In: SPE/IATMI Asia Pacific oil and gas conference and exhibition. Society of Petroleum Engineers

Salehian M, Soleimani R (2018) Development of integrated capacitance resistive model for predicting waterflood performance: a study on formation damage. Energy Sour Part A Recovery Util Environ Eff 40:1814–1825

Salehian M, Temizel C, Gok IM, Cinar M, Alklih MY (2018) Reservoir management through characterization of smart fields using capacitance–resistance models. In: Abu Dhabi International petroleum exhibition and conference. Society of Petroleum Engineers

Sayarpour M (2008) Development and application of capacitance–resistive models to water/carbon dioxide floods. The University of Texas at Austin, Austin

Sayarpour M, Kabir CS, Lake LW (2009) Field applications of capacitance–resistance models in waterfloods. SPE Reserv Eval Eng 12:853–864

Soeriawinata T, Kelkar M (1999) Reservoir management using production data. In: SPE mid-continent operations symposium. Society of Petroleum Engineers

Soroush M, Kaviani D, Jensen JL (2014) Interwell connectivity evaluation in cases of changing skin and frequent production interruptions. J Petrol Sci Eng 122:616–630

Temizel C, Salehian M, Cinar M, Gok IM, Alklih MY (2018) A theoretical and practical comparison of capacitance–resistance modeling with application to mature fields. In: SPE Kingdom of Saudi Arabia annual technical symposium and exhibition. Society of Petroleum Engineers

Thakur GC, Satter A (1998) Integrated waterflood asset management. PennWell Books, Tulsa

Weber DB (2009) The use of capacitance–resistance models to optimize injection allocation and well location in water floods. The University of Texas at Austin, Austin

Weber D, Edgar TF, Lake LW, Lasdon LS, Kawas S, Sayarpour M (2009) Improvements in capacitance–resistive modeling and optimization of large scale reservoirs. In: SPE western regional meeting. Society of Petroleum Engineers

Yousef AA, Lake LW, Jensen JL (2006) Analysis and interpretation of interwell connectivity from production and injection rate fluctuations using a capacitance model. In: SPE/DOE symposium on improved oil recovery. Society of Petroleum Engineers

Zhang Z, Li H, Zhang D (2015) Water flooding performance prediction by multi-layer capacitance–resistive models combined with the ensemble Kalman filter. J Petrol Sci Eng 127:1–19

Zhang Z, Li H, Zhang D (2017) Reservoir characterization and production optimization using the ensemble-based optimization method and multi-layer capacitance–resistive models. J Petrol Sci Eng 156:633–653